Surface & Coatings Technology 213 (2012) 307–312

Contents lists available at SciVerse ScienceDirect

Surface & Coatings Technology

journal homepage: www.elsevier.com/locate/surfcoat

Fabrication and degradation behavior of micro-arc oxidized biomedical magnesium alloy wires

C.L. Chu [a,c,*], X. Han [a,c], J. Bai [a,c], F. Xue [a,c], P.K. Chu [b]

[a] School of Materials Science and Engineering, Southeast University, Nanjing, 211189, China
[b] Department of Physics and Materials Science, City University of Hong Kong, Tat Chee Avenue, Kowloon, Hong Kong, China
[c] Jiangsu Key Laboratory for Advanced Metallic Materials, Southeast University, Nanjing, 211189, China

ARTICLE INFO

Article history:
Received 12 October 2012
Accepted in revised form 31 October 2012
Available online 8 November 2012

Keywords:
Magnesium
Micro-arc oxidation
Composite coating
Degradation behavior

ABSTRACT

A composite ceramic coating containing zirconium is prepared by micro-arc oxidation (MAO) of magnesium alloy wires in a silicate–phosphate composite electrolyte modified with zirconium salts and sodium hydroxide. The effects of the NaOH content in the electrolyte on the microstructure and corrosion resistance of the composite ceramic coating are determined and the degradation behavior is investigated in both simulated body fluid (SBF) and simulated intestinal fluid (SIF). By adding an appropriate amount of NaOH to the composite electrolyte with K_2ZrF_6, the arcing voltage can be reduced and the surface flatness, pore size, and surface coating thickness can be effectively regulated to improve the corrosion resistance. The composite ceramic coating composed of MgO, $MgSiO_3$, and a small amount of ZrO_2 retards surface degradation in both the SBF and SIF environments at different pH values.

1. Introduction

Magnesium alloy is an ideal biodegradable metal [1–4] and wires made of magnesium alloys can replace traditional medical metal wires made of titanium alloys and stainless steels in the development of bioabsorbable gastrointestinal stents, cardiovascular stents, and orthopedic fixation devices. After surgery and healing, the magnesium made devices under spontaneous degradation can circumvent long-term biological safety risks *in vivo* and eliminate the need for a second surgery to remove the biomedical implant. In spite of these advantages, magnesium alloys have poor corrosion resistance and suffer from degradation that is too rapid in the physiological environment thereby limiting medical acceptance [5,6]. Surface modification is a viable approach to improve surface corrosion resistance [7–12] and micro-arc oxidation (MAO) is one of the potential techniques [13–18]. There are both scientific and technical interests in investigating the effects of MAO on the microstructure of the ceramic coating as well as on the corrosion resistance and biological performance of medical magnesium alloy wires, although a systematic study has not been conducted.

The strength, toughness, and corrosion resistance of the MAO ceramic coatings produced using the traditional silicate or phosphate electrolyte system need further improvement. In order to improve the properties of the ceramic coatings, not only the processing parameters but also the electrolyte used in MAO must be optimized. For instance, by adding zirconia nanoparticles [16] or zirconium salts [17,18] to the electrolyte, the mechanical properties and corrosion resistance of the ceramic coatings can be improved due to the introduction of the ZrO_2 phase. In this work, K_2ZrF_6 salts and sodium hydroxide are incorporated into the silicate–phosphate composite electrolyte in order to reduce the micro-arc oxidation arcing voltage and improve the microstructure and properties of the ceramic coatings on magnesium alloy wires. The effects of the NaOH content in the electrolyte on the microstructure and corrosion resistance of the composite ceramic coating containing zirconium are investigated systematically. The ensuing degradation behavior in both simulated body fluid (SBF) and simulated intestinal fluid (SIF) is investigated.

2. Experimental details

2.1. Micro-arc oxidation

AZ31B magnesium alloy wires with a diameter of 0.30 mm were drawn, annealed, gently milled with 2000# SiC sandpaper, washed with acetone, distilled water and ethanol respectively, and subjected to ultrasonic cleaning three times. The WHD-30 type MAO was used with the magnesium alloy wire serving as the anode and the stainless steel sink as the cathode. The samples were suspended in the electrolyte and underwent MAO using different processing parameters. The electrolyte was maintained at 20 to 40 °C by water cooling. After MAO for a predetermined time, the specimens were removed after the power was turned off and washed with deionized water.

* Corresponding author. Tel./fax: +86 25 52090685.
E-mail address: clchu@seu.edu.cn (C.L. Chu).

0257-8972/$ – see front matter © 2012 Elsevier B.V. All rights reserved.
http://dx.doi.org/10.1016/j.surfcoat.2012.10.078

Based on our preliminary studies, the composite electrolyte composed of sodium silicate (10 g/L), sodium phosphate (5 g/L), and K_2ZrF_6 (3 g/L) was used. The sodium hydroxide concentration in the electrolyte was varied from 1 to 4 g/L. The constant voltage mode was used with the forward voltage being 400 V and the negative voltage being 40 V. The oxidation time was 15 min.

2.2. Microstructural characterization

The Bruker D8-Discover X-ray diffractometer (XRD) was used in the phase analysis. The experimental conditions were as follows: Cu-Kα radiation, wavelength of 0.15418 nm, acceleration voltage of 40 kV, current of 30 mA, scanning step of 0.02°/step, scanning speed of 2 s/step, and measured angle error of less than ±0.01°. The Philips XL30 FEG scanning electron microscope (SEM) and FEI SIRION field-emission SEM were used to characterize the surface morphology and thickness of the coatings. The elemental composition was determined by energy-dispersive X-ray spectroscopy equipped on the SEM. The Philips XL30 FEG SEM was used to acquire five random photographs of the surface morphology from each sample (1000×). The Image-Pro software was employed to measure the pore diameters in the SEM photographs. The diameters of 20 to 30 random pores in each photograph were measured and the average pore diameter of all five photographs was taken to represent the pore size of each sample surface. Meanwhile, the region with a black-and-white contrast between 50 and 199 in the photograph was selected as the flat area. The percentage of the flat area in the total area was calculated and the average value of all five photographs was taken to represent the surface flatness of each sample surface.

2.3. Electrochemical measurements

The Princeton Applied Search (PAR) PARSTAT2273 electrochemical workstation was used in the potentiodynamic polarization tests. In the three-electrode system, the saturated calomel electrode was the reference electrode, the platinum foil served as the auxiliary electrode, the sample constituted the working electrode, and the simulated body fluid (SBF) was the corrosion medium. The scanning interval started at a corrosion potential below 250 mV and terminated at higher than 800 mV and the scanning speed was 1 mV/s. In general, the smaller the corrosion current density, the more positive was the corrosion potential and the better the resistance to uniform corrosion.

2.4. Immersion tests

2.4.1. SBF immersion test

Magnesium alloy wires 3 cm long were used in the SBF immersion test. Each wire was placed in a polyethylene bottle containing 15 mL of SBF. It was put in a thermostat oscillation slot at 37.5 ± 0.5 °C. The immersion time lasted from 1 day to 90 days. The soaked SBF was replaced by a fresh one once everyday. After soaking for the preset days, the magnesium alloy wires were taken out from the bottle and the pH of the SBF was measured. The surface morphology and phase composition of the soaked magnesium alloy wires were also evaluated.

2.4.2. SIF immersion test

6.8 g of KH_2PO_4 was dissolved in 250 g of distilled water and then 190 mL of 0.2 mol/L NaOH and 400 mL of distilled water were added. Two kinds of SIF with pH values of 3 and 7 were obtained by introducing diluted HCl and NaOH. The magnesium alloy wire 3 cm long was placed in a polyethylene bottle containing 15 mL of SIF with different pH values and agitated in a thermostatic oscillation slot at 37.5 ± 0.5 °C for 28 days. The surface morphology and phase composition of the soaked magnesium alloy wires were evaluated.

3. Results and discussion

3.1. Microstructure of MAO composite coatings

Fig. 1 depicts the photographs of the magnesium alloy wire before and after MAO. After MAO, the magnesium alloy wire is covered by a white and uniform protective ceramic coating. In the absence of NaOH but using the same electrical parameters, the arcing voltage is higher than 240 V but it is reduced to less than 200 V after adding sodium hydroxide. The growth of the ceramic coating is accelerated with NaOH and the thickness of the composite ceramic coating also increases, as shown in Fig. 2. With increasing NaOH concentration, the conductivity of the electrolyte is improved and the arc voltage is decreased. At the same pulsed voltage, the breakdown pulse energy of the film increases and the breakdown effect becomes more intense. At the same time, the oxide participating in the melting and

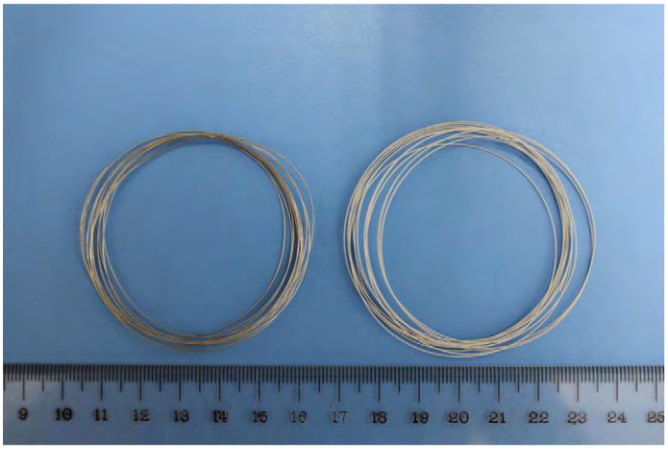

Fig. 1. Photographs of (right) an untreated magnesium alloy wire and (left) a magnesium wire with the MAO composite ceramic coating.

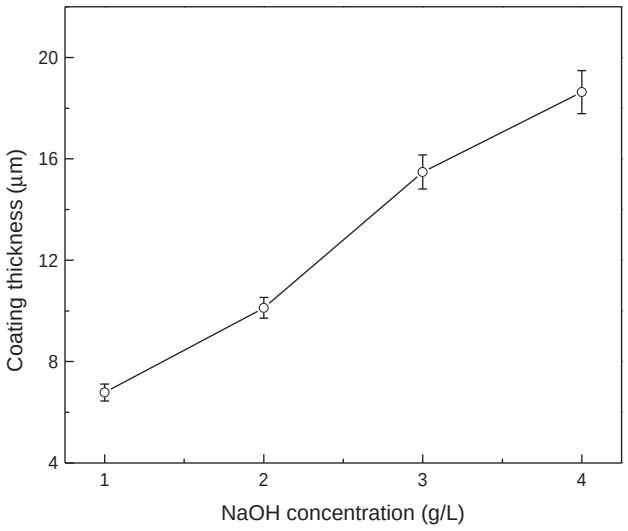

Fig. 2. Thicknesses of the MAO composite coatings on magnesium alloy wires treated with different NaOH concentrations in the electrolyte.

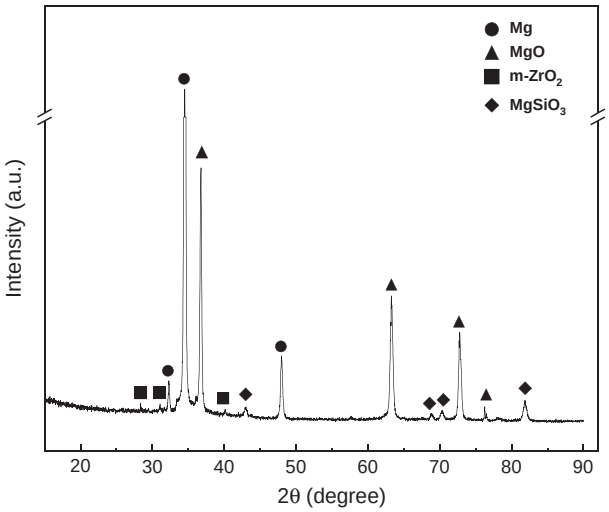

Fig. 3. XRD spectrum of MAO composite coatings on magnesium alloys.

sintering processes gradually increases leading to increased oxidation rate and thicker film. Our data show that the thickness of the composite coating can be changed by varying the amount of NaOH in the electrolyte.

Fig. 3 presents the XRD pattern of the magnesium alloy wire with the MAO composite coating containing zirconium. In addition to the magnesium phase, some MgO and $MgSiO_3$ phases together with a small amount of monoclinic ZrO_2 phase are observed, but there is no MgF_2 phase [18]. This phenomenon is similar to that in another study [17]. During MAO, elements from both the magnesium substrate and electrolyte are involved and incorporated into the oxide.

Table 1
Surface pore size and flatness of the MAO composite coatings on magnesium alloy wires treated with different NaOH concentrations in the electrolyte.

NaOH concentration (g/L)	0	1	2	3	4
Average pore size (μm)	3.06 ± 0.15	2.32 ± 0.09	2.82 ± 0.13	3.37 ± 0.15	2.73 ± 0.11
Surface flatness (%)	59.79 ± 2.65	77.82 ± 3.10	67.82 ± 2.93	57.37 ± 2.86	52.16 ± 2.78

The negatively charged $Zr(OH)_4$ particles derived from zirconium salts in an alkaline solution have important effects on the MAO process [19,20]. Specifically, in the electrolyte system composed of Na_3SiO_4–Na_3PO_4, K_2ZrF_6 reacts with the hydroxyl groups (OH^-) to form white $Zr(OH)_4$ particles. The negatively charged $Zr(OH)_4$ particles under alkaline conditions drift towards the samples and adhere onto the samples under the electric field. They are dehydrated and sintered into the ZrO_2 phase and deposited onto the specimen surface in the high-temperature and high-pressure environment in MAO. The presence of the ZrO_2 phase modulates the surface morphology of the coating by filling or repairing the micro-arc oxidation holes. Fig. 4 exhibits the surface morphology of the composite ceramic coatings after MAO in electrolytes containing various concentrations of NaOH. The average pore size and surface flatness are listed in Table 1. Compared to the results obtained without NaOH, the surface of the sample oxidized in the presence of a small amount of NaOH (1–2 g/L) in the electrolyte shows a relatively high surface flatness of more than 60% and the average surface pore size is less than 3 μm.

As the NaOH concentration is increased to 3 g/L, the quantity and size of the pores increase gradually. Some pores aggregate to form larger interconnected pores. This may be attributed to the increased

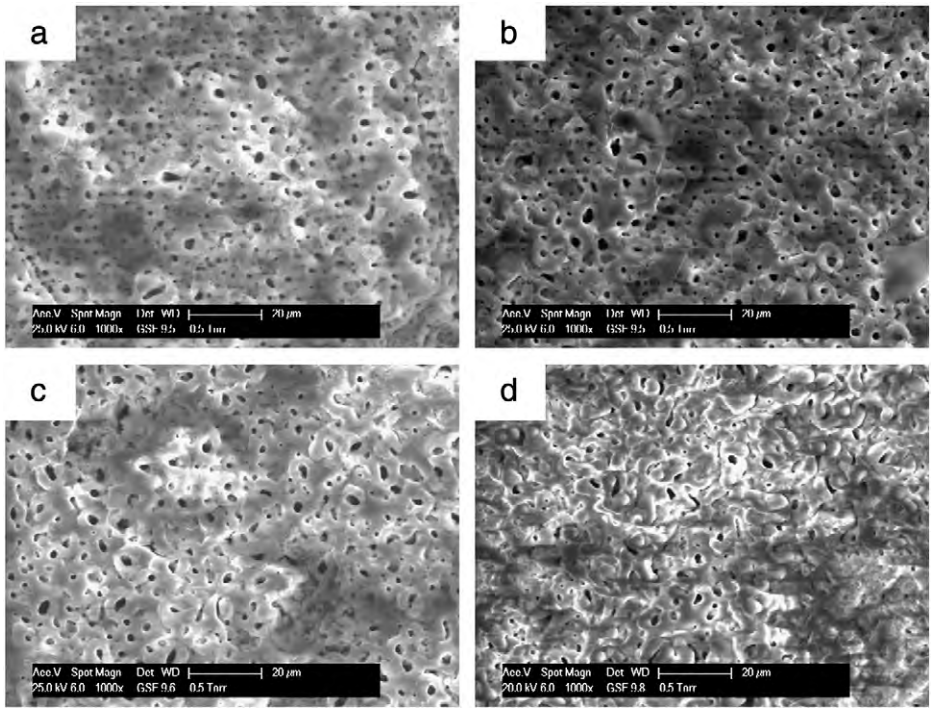

Fig. 4. Surface morphology of the MAO composite coatings on magnesium alloy wires treated with different NaOH concentrations in the electrolyte: (a) 1 g/L, (b) 2 g/L, (c) 3 g/L, and (d) 4 g/L.

conductivity of the electrolyte by adding NaOH. As the conductivity of the electrolyte increases, the sparks generated in the oxidation reaction increases and the number of micro-arcs per unit time goes up. When the NaOH concentration is 4 g/L, the reaction is more severe and the ceramic phases deposited near the micro-arc oxidation volcanic cone begin to stack producing a rougher surface. The surface flatness is reduced while the average pore size decreases. This may stem from the negatively charged $Zr(OH)_4$ particles derived from the reaction between K_2ZrF_6 and the hydroxyl groups (OH^-) [19,20]. As the NaOH content is increased further, the amount of negatively charged $Zr(OH)_4$ particles increases. The $Zr(OH)_4$ particles are prone to directional movement and migrate to the anode region under the electric field. They repair the MAO pores *via* sintering condensation and as a result, the average pore size diminishes.

3.2. Effects of MAO composite coatings on corrosion and degradation behavior

Fig. 5 shows the potentiodynamic polarization curves of the magnesium alloy wires treated with different NaOH concentrations in the electrolytes. The corresponding corrosion potential and corrosion current density are listed in Table 2. The samples show no obvious difference in the corrosion potential. However, after adding sodium hydroxide, the samples have a lower corrosion current density, especially the one treated with 2 g/L of NaOH. The composite ceramic coatings fabricated in the presence of NaOH show slower corrosion.

Two different protective coatings are fabricated using two different electrolytes with and without zirconium salts. The first one is the common MAO coating without zirconium and the second one is a composite MAO coating containing zirconium. The degradation behavior in the simulated physiological environment is evaluated both visually and by SEM. After immersion in SBF, the surface morphology of each sample changes. After 28 days, most of the coatings are intact and uniform although some partial breakage can be observed. After immersion for about 40 days, some magnesium alloy wires with the composite coating are also broken, indicating that degradation occurs for both types of MAO wires during immersion in SBF.

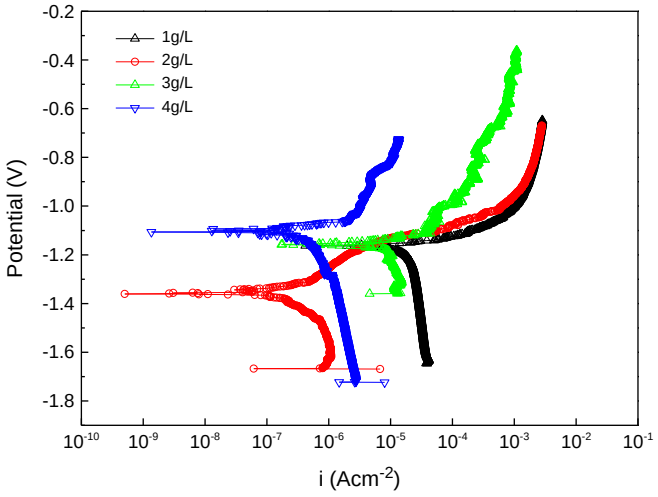

Fig. 5. Potentiodynamic polarization curves of magnesium alloy wires with the composite coatings using different NaOH concentrations in the electrolyte: (a) 1 g/L, (b) 2 g/L, (c) 3 g/L, and (d) 4 g/L.

Table 2
Potentiodynamic polarization analysis of the magnesium alloy wires with composite coatings using different NaOH concentrations in the electrolytes.

NaOH concentration (g/L)	0	1	2	3	4
E_{corr} (V)	−1.23	−1.16	−1.36	−1.16	−1.11
i_{corr} (μA/cm^2)	12.3	2.07	0.26	7.13	1.11

Fig. 6 shows the surface morphology of the two sets of MAO wires with different coatings after immersion for different times in SBF. After immersion for 4 days, both specimens show no corrosion cracking, but after 7 days, some cracks are observed from the common coating (without Zr) but not on the composite coating (with Zr). After immersion for 28 days, the cracks on the common coating surface become larger and more abundant and some white sediment is enriched on its surface. At this time, some cracks also appear from the composite coating but relatively speaking, the corrosion resistance of the composite ceramic coating is better.

The pH impacts the corrosion resistance of the implant materials in the physiological environment. Although the physiological pH is 7.4, the pH values in some parts of the body can vary. For example, the gastric juice in the stomach is strong and has a pH value of 1 to 3 and the pH in the intestinal fluid changes from 3 to 8. Based on the results of the immersion tests in SBF, immersion tests are also conducted in two different SIFs at pH values of 3 and 7 in order to systematically evaluate the corrosion and degradation behavior in different pH environments. Fig. 7 shows the surface morphology of the two MAO magnesium alloy wires with the common coating and composite coating after 28 days of immersion in SIF at a pH value of 7. Corrosion and degradation can be observed from the common coating and the corrosion products cluster on the surface. On the other hand, the surface of the composite coating is smooth and no significant corrosion can be observed.

If the pH of the SIF is adjusted to 3, the improvement rendered by the composite coating containing zirconium pertaining to the corrosion resistance is even more significant. During the early stage (4 days after immersion in SIF at pH = 3), some colorless crystalline substance can be observed from the common coating and the sample becomes brittle. When the samples are removed after immersion for more than 14 days, some of them rupture due to the brittleness caused by corrosion. In comparison, the composite coating exhibits good corrosion resistance in an acidic medium. Sample embrittlement is not obvious and no colorless crystalline substance can be observed.

The surface characteristics of the two kinds of magnesium alloy wires after immersion for the same time in SIF at pH = 3 are significantly different. For instance, the surface morphology of the two samples after immersion for 4 days and 28 days is depicted in Fig. 8. Comparing Fig. 8a and b, some crystalline substance emerges on the surface of the common coating very quickly but it is not so on the composite coating. This is consistent with our visual observation. Fig. 9 shows that the main phase of the colorless crystalline substance shown in Fig. 8a is $MgHPO_4 \cdot 3H_2O$ which is generated by the reaction between magnesium or magnesium oxide and the free HPO_4^{2-} groups in the acidic medium. Although the $MgHPO_4 \cdot 3H_2O$ covering on the sample surface has a certain degree of corrosion inhibition effect, as the corrosion reaction proceeds, continuous consumption of magnesium oxide and magnesium makes the MAO ceramic coating thinner and the magnesium wire finer, ultimately leading to complete erosion.

After soaking in the acidic SIF environment at a pH value of 3 for 28 days, the surface of the common coating is rough and uneven. The crystalline substance produced in the early immersion stage disappears. Instead, a large number of corrosion pits and trenches emerge from the wire. In comparison, the wire with the composite

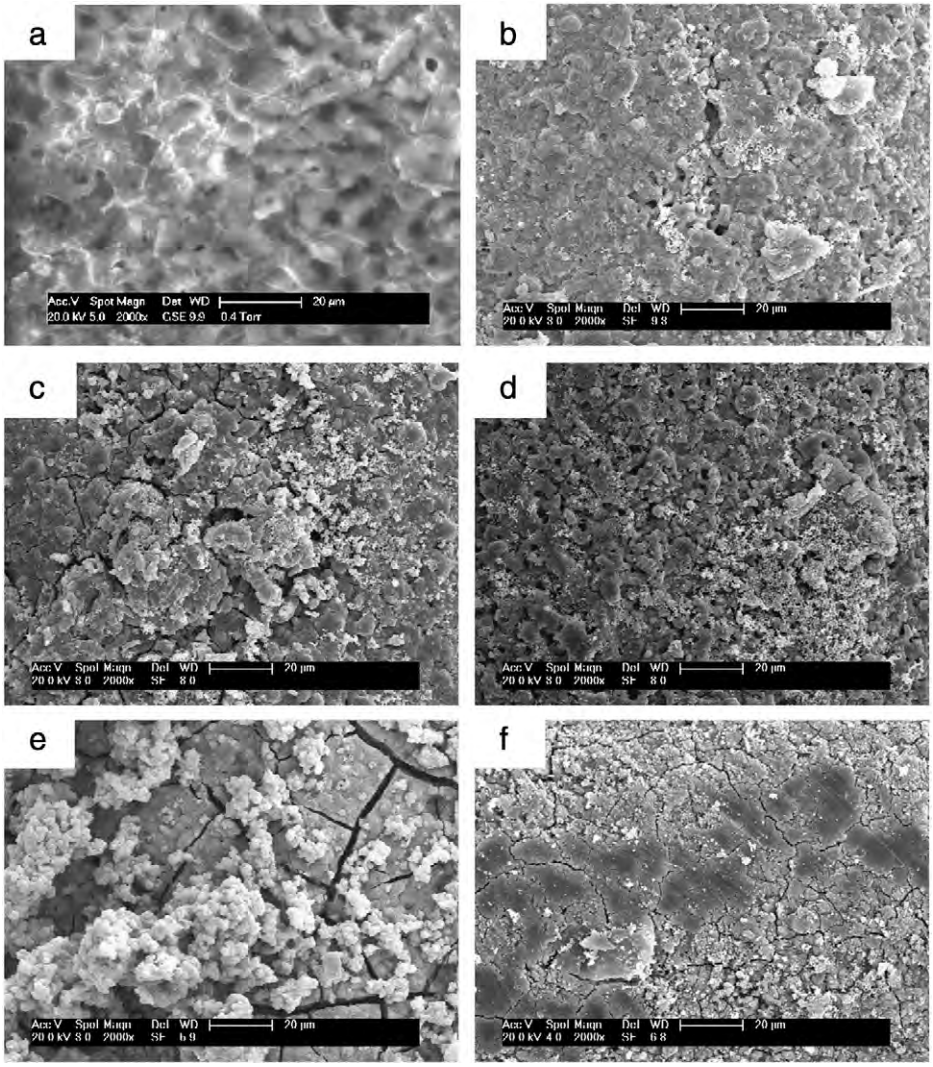

Fig. 6. Surface morphology of the MAO-treated magnesium alloy wires with different coatings after immersion in SBF for different times: (a) common coating without Zr, 4 days; (b) composite coating with Zr, 4 days; (c) common coating, 7 days; (d) composite coating, 7 days; (e) common coating, 28 days; (f) composite coating, 28 days.

coating containing zirconium shows a smaller corrosion rate and is less vulnerable to corrosion. This is because the ZrO_2 phase improves the corrosion resistance, mechanical properties, and adhesion of the MAO ceramic coating.

4. Conclusion

Incorporation of an appropriate amount of NaOH into the silicate–phosphate electrolyte containing K_2ZrF_6 salt reduces the arcing

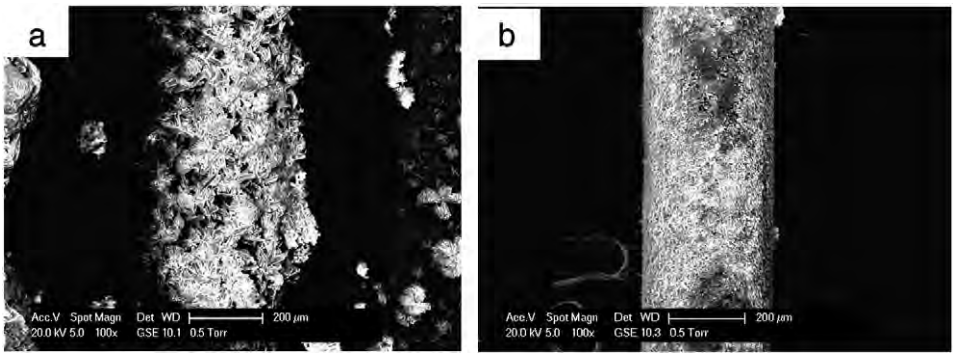

Fig. 7. Surface morphology of the two MAO-treated magnesium alloy wires: (a) common coating and (b) composite coating after immersion in SIF for 28 days at a pH value of 7.

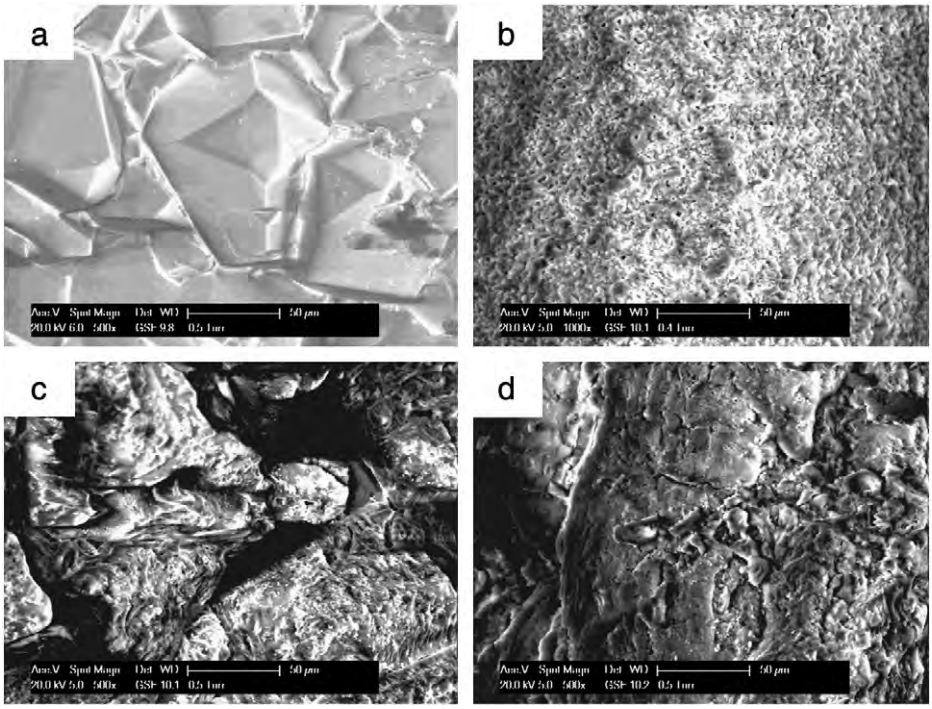

Fig. 8. Surface morphology of the MAO-treated magnesium alloy wires with different coatings after immersion in SIF at a pH value of 3: (a) common coating, 4 days; (b) composite coating, 4 days; (c) common coating, 28 days; (d) composite coating, 28 days.

voltage in MAO and accelerates the oxidation rate. The surface flatness and pore size of the composite coating are altered and as a result, the corrosion resistance is enhanced. The composite coating fabricated on the magnesium alloy wires in the composite electrolyte containing K_2ZrF_6 salt and NaOH is composed of MgO and $MgSiO_3$ together with a small amount of ZrO_2. In comparison with the MAO coating without Zr, the composite coating with Zr offers better protection against corrosion and retards surface degradation on the magnesium alloy wires in different simulated physiological environments including simulated body fluid and simulated intestinal fluid at pH values of 3 and 7.

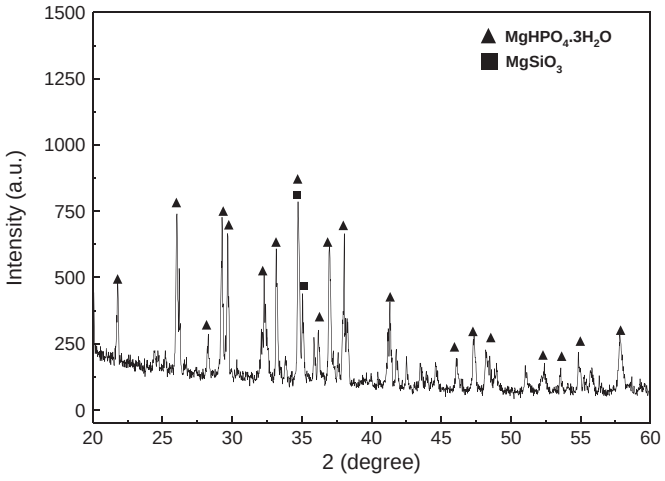

Fig. 9. XRD spectrum of the MAO-treated magnesium alloys with the common coating after immersion in SIF for 4 days at a pH value of 3.

Acknowledgments

This work was financially supported by the Science and Technology Support Program of Jiangsu Province (BE2011778), Hong Kong Research Grants Council (RGC) General Research Funds (GRF) nos. CityU 112510 and 112212, and City University of Hong Kong Applied Research Grant (ARG) 9667066.

References

[1] F. Witte, Acta Biomater. 6 (2010) 1680.
[2] M.P. Staiger, A.M. Pietak, J. Huadmai, G. Dias, Biomaterials 27 (2006) 1728.
[3] Y. Zong, G.Y. Yuan, X.B. Zhang, L. Mao, J.L. Niu, W.J. Ding, Mater. Sci. Eng. B 177 (2012) 395.
[4] T. Kraus, S.F. Fischerauer, A.C. Häzi, P.J. Uggowitzer, J.F. Löfler, A.M. Weinberg, Acta Biomater. 8 (2012) 1230.
[5] X.N. Gu, Y.F. Zheng, Y. Cheng, S.P. Zhong, T.F. Xi, Biomaterials 30 (2009) 484.
[6] Y. Xin, T. Hu, P.K. Chu, Acta Biomater. 7 (2011) 1452.
[7] H. Hornberger, S. Virtanen, A.R. Boccaccini, Acta Biomater. 8 (2012) 2442.
[8] C. Wen, S. Guan, L. Peng, C. Ren, X. Wang, Z. Hu, Appl. Surf. Sci. 255 (2009) 6433.
[9] H.M. Wong, K.W.K. Yeung, K.O. Lam, V. Tam, P.K. Chu, K.D.K. Luk, et al., Biomaterials 31 (2010) 2084.
[10] L. Xu, F. Pan, G. Yu, L. Yang, E. Zhang, K. Yang, Biomaterials 30 (2009) 1512.
[11] K.Y. Chiu, M.H. Wong, F.T. Cheng, H.C. Man, Surf. Coat. Technol. 202 (2007) 590.
[12] C. Wu, Z. Wen, C. Dai, Y. Lu, F. Yang, Surf. Coat. Technol. 204 (2010) 3336.
[13] X.N. Gu, N. Li, W.R. Zhou, Y.F. Zheng, X. Zhao, Q.Z. Cai, et al., Acta Biomater. 7 (2011) 1880.
[14] P.B. Srinivasan, J. Liang, C. Blawert, M. Stomer, W. Dietzel, Appl. Surf. Sci. 256 (2010) 4017.
[15] C.E. Barchiche, E. Rocca, C. Juers, J. Hazan, J. Steinmetz, Electrochim. Acta 53 (2007) 417.
[16] R. Arrabal, E. Matykina, P. Skeldon, G.E. Thompson, J. Mater. Sci. 43 (2008) 1532.
[17] Z.P. Yao, H.H. Gao, Z.H. Jiang, F.P. Wang, J. Am. Ceram. Soc. 91 (2) (2008) 555.
[18] W.Y. Mu, Y. Han, Surf. Coat. Technol. 202 (2008) 4278.
[19] S.G. Xin, R.R. Zhao, H. Du, J. Inorg. Mater. 24 (1) (2009) 107.
[20] Y.F. Xu, W.Y. Fan, China Powder Technol. 6 (S1) (2000) 251.